



# OPEN High-dose IL-37 promotes inflammatory activity of macrophage via Preferential ligation of the IL-18R $\alpha$

Yu Zhang<sup>1</sup>✉, Beixi Shi<sup>1</sup>, Yaxin Bi<sup>2</sup>, Xiaxin Wu<sup>1</sup>, Xiangning Li<sup>1</sup>, Jinfeng Wu<sup>1</sup>, Jiahui Qiu<sup>1</sup>, Zhijie Lin<sup>3</sup>, Guotao Lu<sup>4</sup> & Weijuan Gong<sup>1,3,5</sup>✉

Interleukin-37 (IL-37) exists in various human tissues and organs and exhibits extensive anti-inflammatory activity. Recombinant IL-37 ameliorates the insulin resistance and inflammation associated with obesity and type 2 diabetes (T2DM). However, the specific role and underlying mechanisms of different doses of IL-37 in macrophage inflammatory response in T2DM remain to be discovered. In our study, we determined the dual role of IL-37 in macrophage inflammatory response both in vitro and vivo. We discovered that very low doses of IL-37 (10 ng/ml in vitro and 100 ng/ml in vivo) are sufficient to elicit significant anti-inflammatory effects. Conversely, high-dose IL-37 promotes the inflammatory response in macrophages. Specifically, a high dose of IL-37 (1000 ng/ml) did not improve blood glucose levels, intraperitoneal glucose tolerance, or insulin tolerance, nor did it reduce the number of islet macrophages in the T2DM model. Mechanistically, our in vitro and in vivo experiments demonstrated that high-dose IL-37 inhibited the activation of key signaling molecules such as phosphatase and tensin homolog (PTEN), AMP-activated protein kinase (AMPK), and signal transducer and activator of transcription 3 (STAT3) via preferential binding to IL-18R $\alpha$  in macrophages. In contrast, low-dose IL-37 resulted in the activation of these signaling pathways. Collectively, these findings highlight low-dose IL-37 as a potential therapeutic agent to ameliorate inflammatory reactions and metabolic disturbances during T2DM. However, it is crucial to note that high-dose IL-37 may have no beneficial effects or could even exacerbate the condition.

**Keywords** IL-37, IL-18R $\alpha$ , Type 2 diabetes, Macrophage, Inflammation

The IL-37 gene is located in the IL-1 family gene cluster (2q13) on the long arm of human chromosome 2, with a length of 3.617 kb<sup>1</sup>. Among the members of the IL-1 family, IL-37 is the only one without a mouse homologue<sup>2</sup>. IL-37 can be divided into five subtypes (IL-37a–e) based on the different exons<sup>3</sup>. Several researchers believe that IL-37a, IL-37b, and IL-37d all contain exons 4–6 and have biological functions<sup>4–6</sup> whereas IL-37c and IL-37e lack exon 4 and cannot encode the secondary structure of  $\beta$ -clover and thus have no biological function<sup>1,5</sup>. IL-37 exists in numerous human tissues and organs, such as the brain, lung, bone marrow, uterus, lymph nodes, thymus, and testis<sup>7</sup>.

IL-37 is a member of the IL-1 family and a cytokine with anti-inflammatory and immunosuppressive functions. IL-37 can transform pro-inflammatory cytokines into anti-inflammatory cytokines, such as regulating lipid metabolism and macrophage polarization<sup>8,9</sup>. Recently, much progress has been made in the anti-inflammatory effect and mechanism of IL-37. Wild-type mice treated with human recombinant IL-37 protein and transgenic mice expressing human IL-37 are not prone to experimental inflammation such as colitis<sup>10</sup> endotoxemic shock, lung and spinal cord injury<sup>11</sup> cardiovascular disease<sup>12</sup> arthritis<sup>13,14</sup> and fatigue<sup>15</sup>. Abnormal expression of IL-37 can be

<sup>1</sup>School of Nursing, Yangzhou University, 136 Jiangyang Road, Yangzhou City 225009, Jiangsu, China. <sup>2</sup>Northern Jiangsu People's Hospital, Yangzhou 225009, Jiangsu, China. <sup>3</sup>Department of Basic Medicine, School of Medicine, Yangzhou University, 136 Jiangyang Road, Yangzhou 225009, Jiangsu, China. <sup>4</sup>Department of Gastroenterology, Affiliated Hospital of Yangzhou University, Yangzhou University, Yangzhou 225009, Jiangsu, China. <sup>5</sup>Jiangsu Key Laboratory of Zoonosis, Jiangsu Co-innovation Center for Prevention and Control of Important Animal Infectious Diseases and Zoonoses, Yangzhou University, Yangzhou, China. ✉email: yizhangyu@yzu.edu.cn; wjgong@yzu.edu.cn

observed in human inflammation and various autoimmune diseases (including psoriasis and systemic lupus erythematosus) to limit the body's excessive inflammatory response<sup>16</sup>.

In recent years, the incidence rate of type 2 diabetes (T2DM) has increased year by year, and has become a global health problem. According to the data of the International Diabetes Federation (IDF), T2DM now affects more than 10% of the adult population, which is expected to increase to 578 million by 2030 and 783.2 million by 2045<sup>17,18</sup>. Current research suggests that immune responses and inflammation may play a role in the pathophysiology of T2DM and its complications<sup>19,20</sup>. Multiple pieces of evidence suggest that targeted drugs for the treatment of inflammation in T2DM are IL1 $\beta$  antagonists, nonsteroidal anti-inflammatory drugs, etc. currently, however, their effects are still unsatisfactory<sup>21</sup> or have significant side effects<sup>22</sup>. Therefore, finding effective measures to reverse the local inflammatory state of T2DM is of great significance for effectively treating T2DM.

Inflammatory stimulation can induce the production of IL-37, a self-protection mechanism against uncontrolled inflammation and excessive tissue damage<sup>23</sup>. Overexpression of IL-37 can restrain the imbalance of intestinal microbiota and the deterioration of diabetes in mouse models<sup>24</sup>. IL-37 can improve insulin resistance and the production of proinflammatory cytokines in adipose tissue induced by a high-fat diet and suppress the activation of AMP-activated protein kinase (AMPK) in macrophages and adipocytes<sup>25,26</sup>. However, the exact mechanism by which IL-37 exerts anti-inflammatory effects to improve obesity and T2DM is currently not fully understood.

It has been demonstrated that IL-37 can form a polymer with IL-1R8 and IL-18Ra, which are indispensable receptors, simultaneously to perform an anti-inflammatory function via triggering a signaling cascade, via activation of PTEN (phosphatase and tensin homolog), and inhibition of the phosphorylation of MAPKs (mitogen-activated protein kinases) and Syk (spleen tyrosine kinase) pathways<sup>27</sup>. Li et al. reported that IL-37d inhibits tumor necrosis factor (TNF)- $\alpha$ -stimulated soluble suppression of tumorigenicity 2 expression via the inactivation of IL-1R8-dependent NF- $\kappa$ B to promote type 2 immune homeostasis in white adipose tissue<sup>28</sup>; thus, it may be a prospective therapeutic target for obesity and other metabolic disorders. But there are currently no relevant reports on the effects and mechanisms of whether IL-37 passes IL-1R8 and IL-18Ra and exerts anti-inflammatory effects to improve T2DM.

A very low dose of IL-37 can inhibit the inflammatory response of macrophages effectively<sup>4,11</sup>. Recombinant IL-37 at a deficient concentration (1 mg per mouse) in vivo is sufficient to exert an ideal and effective anti-inflammatory effect<sup>4,26</sup>. However, IL-37 with high concentrations has weak inhibitory effects on the release of inflammatory cytokines<sup>29</sup>. Our team unexpectedly found that the proinflammatory activity of high-dose IL-37 was significantly enhanced, and there was no good therapeutic effect on the T2DM mouse model, but the exact mechanism of this phenomenon is still unclear. Therefore, this study aims to further clarify the exact role and specific mechanism of high and low dose IL-37 in the T2DM model, lay the foundation for clinical development of new T2DM anti-inflammatory drugs with dose effect, and provide guidance for individualized treatment of diabetes.

## Materials and methods

The study involving human participants complied with the Declaration of Helsinki and was approved by the Ethics Committee of Medical College of Yangzhou University. All participants signed an informed consent form. The animal study was also reviewed and approved by the Ethics Committee of Medical College of Yangzhou University. All the methods were performed in accordance with the ARRIVE guidelines. The reference number is YXYLL-2020-68.

### Animals

Male SPF C57BL/6 WT mice aged 3 weeks and weighing > 15 g were purchased from the Comparative Medicine Centre of Yangzhou University (Yangzhou, China), and the same 3-week-old IL-37 TG male mice were provided by Nanjing General Hospital (Nanjing, China). They were acclimatized and fed with clean drinking water and food as usual in the laboratory animal room of the School of Nursing, Yangzhou University (Yangzhou, China). The mice were fed with conventional diets until eight weeks of age to conduct animal experiments. At the end of the experiment, mice were anesthetized with pentobarbital (50 mg/kg) and then euthanized by decapitation in accordance with the ARRIVE guidelines. All animal experiments were approved by the Ethics Committee of Medical College of Yangzhou University (YXYLL-2020-68) and were performed in accordance with the guidelines for animal experiments.

### Sample collection

The subjects were enrolled from the Affiliated Hospital of Yangzhou University (Yangzhou First People's Hospital) and were approved by the Ethics Committee of Medical College of Yangzhou University (YXYLL-2020-68). All participants signed an informed consent form. T2DM patients and healthy people were recruited into this study. After overnight fasting for 12 h, 5 ml venous blood samples were collected from each of the T2DM patients ( $n = 11$ ) and healthy people ( $n = 14$ ). After acquisition, the specimens were transferred to the laboratory in an ice box as soon as possible, and all samples were stored at

– 4 °C until analysis.

### Experimental design

The WT mice were divided into WT-normal, WT-T2DM, 100 ng/ml rIL-37 treatment, 1000 ng/ml rIL-37 treatment, metformin treatment, and liraglutide treatment groups, with a total of six groups consisting of 5 mice each. The animals were acclimatized and fed for 2 weeks. The WT-normal group was started with normal mouse chow, and the modeling group was given a 45% high-fat diet (Research Diets Inc, New Brunswick, USA). Then,

85 mg/kg STZ (Sigma, Lenexa, USA) was injected intraperitoneally twice at an interval of 3 days on the 4th week (with overnight fasting for 12 h before STZ injection). At three days after the injection, fasting was conducted for 12 h, and 60 µl blood samples were obtained from the tail vein; mice with blood glucose  $\geq 11.1$  mmol/L were considered to be successful in T2DM modeling<sup>30</sup>. The WT-normal group was fed with normal mouse chow, and the WT model group was fed with a 45% high-fat diet for 3 weeks. The body weight and glucose were monitored regularly during the feeding period.

After the completion of two injections of STZ on the 4th week, the intervention was started. The WT-T2DM group was given intraperitoneal injection of 0.2 ml/each PBS, the metformin (Sino-US Shanghai Squibb Pharmaceutical Co., Shanghai, China) group was given intraperitoneal injection of 200 mg/(kg·day) metformin<sup>31</sup> and the liraglutide (Novo Nordisk Research Diets, Beijing, China) group was intraperitoneally injected with 0.2 mg/(kg·day) liraglutide<sup>32</sup>. The 100 and 1000 ng/ml rIL-37 treatment groups were intraperitoneally injected with 100 and 1000 ng/mouse rIL-37 (Peprotech, New Jersey, USA), respectively. The metformin, liraglutide, and WT-normal groups were injected daily, whereas the WT-T2DM and rIL-37 treatment groups were injected weekly. IPGTT and ITT experiments were performed at the end of the 6th week. At the end of the 7th week, all mice were fasted for 12 h. Then, 50 µl blood was collected to assess the overall level of glucose in the plasma and mouse pancreas, and spleen and peripheral blood were obtained for flow analysis. Fig.S1 shows the detailed modeling and intervention process.

### RT-PCR

RNA was extracted from a 3 mm piece of mouse tail using Trizol in accordance with the manufacturer's instructions (Invitrogen™, ThermoScientific, UK). cDNA was synthesized using SuperScript II Reverse Transcriptase (200U), and approximately 300 ng RNA and random hexamer primers (150 ng, Invitrogen™, ThermoScientific, UK) were used. GAPDH was used as the internal control. The primers are as follows: IL37-F: 5'-CAGTACATCAATGGGCGTGGA-3' and IL37-R: 5'-CTTCAC CTTTGGACTTGTGTGAAC-3'. PCR amplification was performed using an ABI GeneAmp PCR System 7500 as follows: 60 °C, 30 min, one cycle; 94 °C for 3 min, one cycle; 94 °C for 30 s, 60 °C for 30 s, and 72 °C for 35 s, 38 cycles; 68 °C for 5 min, one cycle. The PCR products were separated using electrophoresis through 1.5% agarose gels. Amplicons were stained with ethidium bromide and visualized using ultraviolet-light transillumination. PCMV6-AC-GFP (Origene, Rockwell, USA)-transfected cells were used as controls.

### Flow cytometry

Single-cell suspensions were prepared from the spleen and peripheral blood of WT and IL-37 TG mice, labeled with flow antibodies F4/80, CD11c, CD16/32, CD206, CD86, CD4, CD8, PDL1, TNF- $\alpha$ , IL18R $\alpha$ , and IL1R8 (Biolegend, California, USA), and detected by BD FACSVerse Flow Cytometer. The assay results were analyzed by Flowjo software.

### Immunohistochemistry

Small pieces of pancreatic tissue were fixed with 4% paraformaldehyde overnight, dehydrated, and paraffin embedded, and 4 µm sections were prepared. Immunohistochemical staining steps included the following: dewaxing of paraffin sections to water first, using 0.01 mol/L citrate buffer for antigen repair, removal of endogenous peroxidase with 3% hydrogen peroxide solution, addition of F4/80 antibody (1:1000), and overnight incubation at 4 °C. The next day, PBS was used to rinse the sections thrice, with each wash lasting for 5 min. The secondary antibody horseradish peroxidase-labeled goat anti-rabbit IgG (1:5000) was added, and the sections were incubated for 15 min at room temperature, rinsed thrice with PBS, and applied with 3,3'-Diaminobenzidine (DAB) for color development. After re-staining, dehydration, transparency and blocking, the slices were observed under a light microscope for image acquisition and analysis.

### Western blot

Single-cell suspensions ( $10^6$  cells) were isolated from the spleen tissue to isolate macrophages. Protein lysates were extracted from the macrophages. Proteins were extracted with radio immunoprecipitation assay lysis buffer with protease and phosphatase inhibitors. The protein concentrations were determined with a BCA protein assay kit. Then, the expression of each protein on the signaling pathways of PTEN/STAT3/AMPK and AKT/Erk/NF- $\kappa$ B/mTOR (Cell Signaling Technology, Boston, USA) were examined by Western blot.

### ELISA

A total of 5 mL fasting venous blood was collected from the patients, placed in ethylene diamine tetraacetic acid anticoagulation tubes, and centrifuged at 3000 r/min for 15 min with a centrifugation radius of 11 cm. Finally, the supernatant was collected, and the concentration of serum IL-37 was detected by the ELISA technique following the instructions of the human IL-37 ELISA kit (Colorful Gene Biological Technology Co, LTD, Wuhan, China).

### Immunofluorescence

The isolated macrophages were distributed to culture dishes, and the density of each well was  $2 \times 10^6$ /L. The above macrophages were treated with different concentrations of IL-37 recombinant protein (0, 10, 100, and 200 ng/ml, which represented the control, low, and high doses, respectively), and cells were collected after 24 h of incubation and rinsed thrice with PBS. The supernatant was removed cleanly, paraformaldehyde fixation was added, and then the mixture was placed in at 4 °C for 30 min. Cell smear was made, closed, and incubated with IL-1R8 primary antibody (Biorbyt, Cambridge, UK) at room temperature with moisturizing shock for 1.5 h. Then, the smear was washed thrice with PBS, followed by secondary antibody incubation at room temperature with moisturizing shock for 10 min, and washed thrice again with PBS. Signal amplification, antibody elution, and

the above steps were repeated for IL-18R $\alpha$  (Abxbexa, Cambridge, UK). Finally, cell nuclei were stained and sealed, and the stained tissue slices were observed and analyzed under a confocal microscope (ZEISS LSM 880NLO).

## 10. Statistical analysis

All data are expressed as means  $\pm$  SEM. The statistical significance of the differences between various treatments or groups was measured by either Student's *t*-test or analysis of variance (ANOVA) followed by the Bonferroni post-test. Data analyses were performed using GraphPad Prism 7.0. *P* < 0.05 was considered statistically significant.

## Results

### More macrophages were observed in IL-37<sup>hi</sup>- Transgenic (TG) mice

First, through reverse transcription-polymerase chain reaction (RT-PCR), we determined that the expression of IL-37 in IL-37<sup>hi</sup>-TG mice was significantly higher than that of IL-37<sup>low</sup>-TG mice, whereas the expression of IL-37 in IL-37<sup>low</sup>-TG mice was slightly higher than that in WT mice (Fig. 1A). Same phenomenon was observed from the results of enzyme-linked immunosorbent assay (ELISA) in serum (Fig. 1B). Then, we further observed the changes in the immune cells of IL-37-TG mice and noticed that the frequencies of F4/80 + and CD11c + cells in IL-37<sup>hi</sup>-TG mice were significantly higher than those in WT mice, whereas no significant difference was identified between IL-37<sup>lo</sup>-TG and WT mice (Fig. 1C). Under the stimulation of lipopolysaccharide (LPS), the expressions of TNF- $\alpha$  (Fig. 1D and E) and CD86 (Fig. 1F) in F4/80 + macrophages of IL-37<sup>hi</sup>-TG mice were significantly higher than those in WT mice, whereas the expression of programmed death-ligand 1 (PDL-1) (Fig. 1G) did not change significantly. In addition, we observed significant increases in the M1 and M2 subsets in IL-37<sup>hi</sup>-TG mice whether they were stimulated by phosphate-buffered saline (PBS) or LPS (Fig. 1H and I). Upregulated numbers and activities of CD8 + T cells were also detected in IL-37<sup>hi</sup>-TG mice (Fig. 1J and Supplementary Fig.S2A–D). We also observed the effects of IL-37 on CD4 + T cells. No significant difference was observed in the frequencies of CD4 + NKG2D + and CD4 + IFN- $\gamma$  + cells between groups (Supplementary Fig. S3A). Enhanced frequencies of CD4 + IL-17 + cells and regulatory T cells were discovered in the IL-37<sup>hi</sup>-TG and IL-37<sup>lo</sup>-TG mice (Supplementary Fig.S3B and S3C), respectively, and 1 ng/ml rIL-37 inhibited the rest of CD4 + IFN- $\gamma$  + cells (Supplementary Fig.S3D). The 1 ng/ml rIL-37 also inhibited IL-2-activating NK1.1 + IFN- $\gamma$  + cells (Supplementary Fig.S4B), and no significant changes were observed in the NK1.1 + NKG2D + cells of IL-37 TG mice (Supplementary Fig.S4A). Moreover, enhanced frequencies of CD3 +  $\gamma\delta$  + NKG2D+ (Supplementary Fig. S5B), CD11b+, and CD11b + Gr-1 + cells (Supplementary Fig.S7A) were found in IL-37<sup>hi</sup>-TG mice. In addition, weakly enhanced frequency of regulatory B cells was discovered in IL-37<sup>lo</sup>-TG mice (Supplementary Fig.S8A).

### High-dose rIL-37 stimulates macrophage activity

To understand the effect of different doses of rIL-37 on macrophages, we stimulated the spleen F4/80 macrophages of WT mice with different concentrations of rIL-37 (0, 1, 10, 100, 200, and 500 ng/ml) and observed that whether before or after LPS stimulation, low-dose rIL-37 (10 ng/ml) inhibited the expressions of TNF- $\alpha$  (Fig. 2A and B) and CD86 (Fig. 2C) significantly, whereas high doses of rIL-37 (100, 200, and 500 ng/ml) showed the opposite or had no effect. No significant change was observed in the F4/80-PD-L1 expression under different rIL-37 doses (Fig. 2D). We also stimulated the spleen CD11c + and CD11b + cells of WT mice with different concentrations of rIL-37, and no significant changes were observed in the CD11c-CD86 (Supplementary Fig.S6A), CD11c-PD-L1 (Supplementary Fig.S6B), and CD11b-PD-L1 (Supplementary Fig.S7B) expressions under different rIL-37 doses.

### High-dose rIL-37 could not reverse T2DM induced by HFD and STZ

To observe the effect of rIL-37 on the experimental T2DM model, we injected rIL-37 intraperitoneally during the construction of the model. We observed that intraperitoneal injection of 100 and 1000 ng/mouse rIL-37 could not change the body weight of the experimental T2DM model significantly (Supplementary Fig.S9). The results showed that 100 ng/mouse rIL-37 decreased the fasting blood glucose level and immunohistochemical staining of F4/80-positive cells in islets of the experimental T2D model effectively, but 1000 ng/mouse rIL-37 did not (Fig. 3A, D). In addition, 100 ng/mouse rIL-37 improved glucose tolerance (intraperitoneal glucose tolerance test (IPGTT)) and insulin tolerance (insulin tolerance test (ITT)) effectively in the experimental T2D model, but 1000 ng/mouse rIL-37 did not (Fig. 3B and C). We collected the peripheral blood of T2DM patients and healthy controls and found an enhanced level of serum IL-37 in patients with T2DM (Fig. 3E).

### High-dose rIL-37 inhibit STAT3 activation of macrophages

To explore the molecular mechanism of different doses of rIL-37 on macrophages, we sorted macrophages from mouse spleen, stimulated them with LPS, and treated them with exogenous rIL-37 (0, 1, 10, 100, and 200 ng/ml). The results suggested that 1 ng/ml or 10 ng/ml rIL-37 was sufficient to promote the activation of PTEN, STAT3, and AMPK $\alpha$  significantly (Fig. 4A and F). However, compared with 1 ng/ml or 10 ng/ml rIL-37, 200 ng/ml rIL-37 inhibited the above genes' activation (Fig. 4A and F). In addition, 1 ng/ml or 10 ng/ml rIL-37 inhibited the expression or activation of AKT, Erk1/2, NF- $\kappa$ B and mTOR effectively, whereas 100 ng/ml or 200 ng/ml rIL-37 reversed the decrease in protein expression or activation caused by 1 ng/ml or 10 ng/ml rIL-37 mentioned above (Fig. 4G and O). To further determine whether the changes in the above proteins and signal pathways were related to the binding and recruitment of IL-37 to IL-18R $\alpha$ /IL-1R8, we added different concentrations of rIL-37 to the spleen macrophages together with PBS and LPS and observed from the immunofluorescence results that high doses of rIL-37(100, and 200 ng/ml) resulted in more expression of IL-18R $\alpha$  than IL-1R8 (Fig. 4P). Flow cytometry experiments also confirmed the above results (Fig. 4Q).



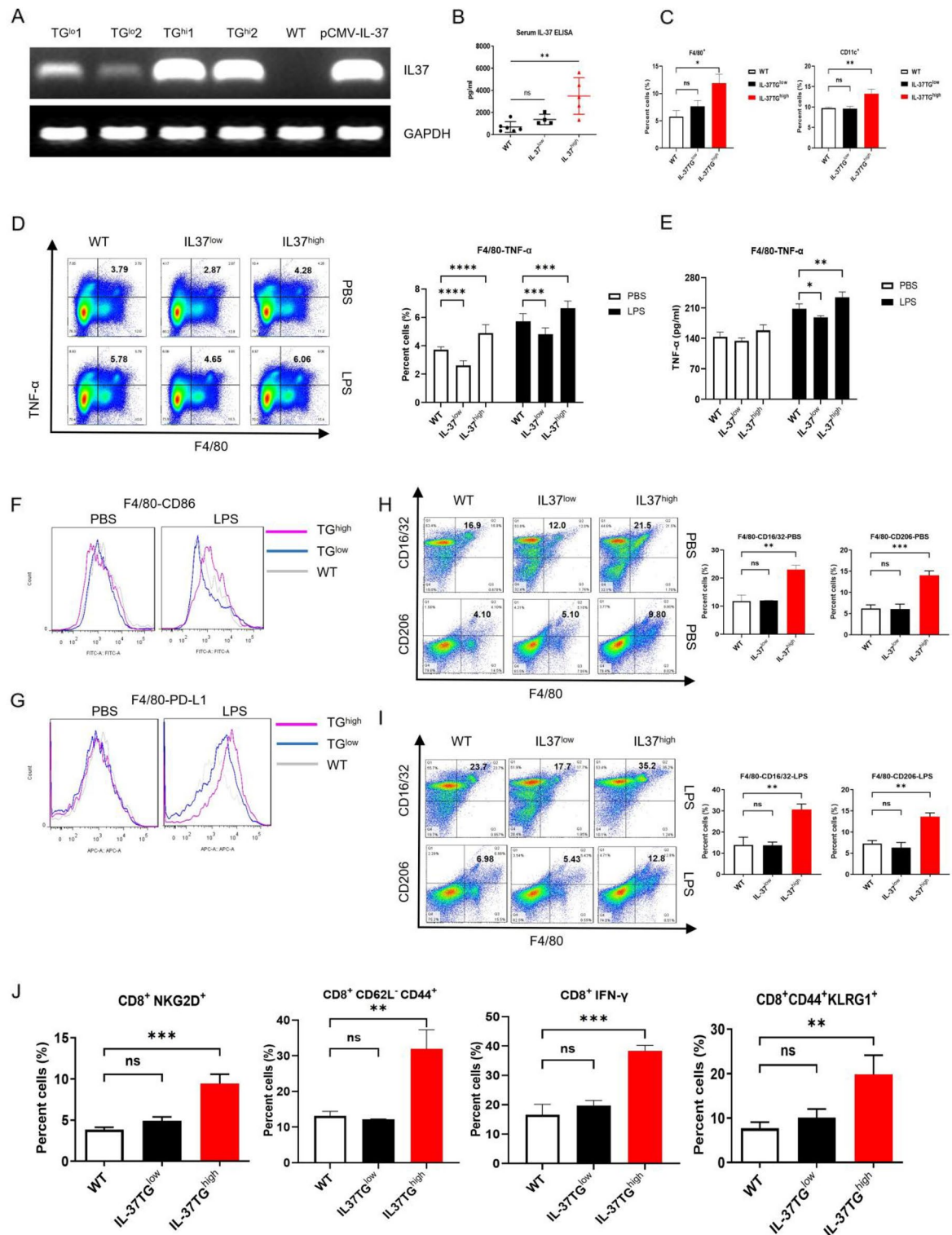


**Fig. 1. Upregulated activities of macrophages in IL-37<sup>hi</sup>-TG mice.** (A, B) Identification of mouse strains with distinct IL-37 expression. (C) Enhanced frequency of F4/80<sup>+</sup> and CD11c<sup>+</sup> cells in IL-37<sup>hi</sup>-TG mice. (D-G) Changes of splenic macrophage activities in IL-37<sup>lo</sup>-TG and IL-37<sup>hi</sup>-TG mice before or after LPS stimulation (F4/80-TNFα, F4/80-CD86, and F4/80-PD-L1, respectively). (H, I) Increased M1 and M2 subsets in IL-37<sup>hi</sup>-TG mice, respectively. (J) Upregulated CD8<sup>+</sup> T cell activities in IL-37<sup>hi</sup>-TG mice. \**P*<0.05, \*\**P*<0.01, \*\*\**P*<0.001, ns: not significant.

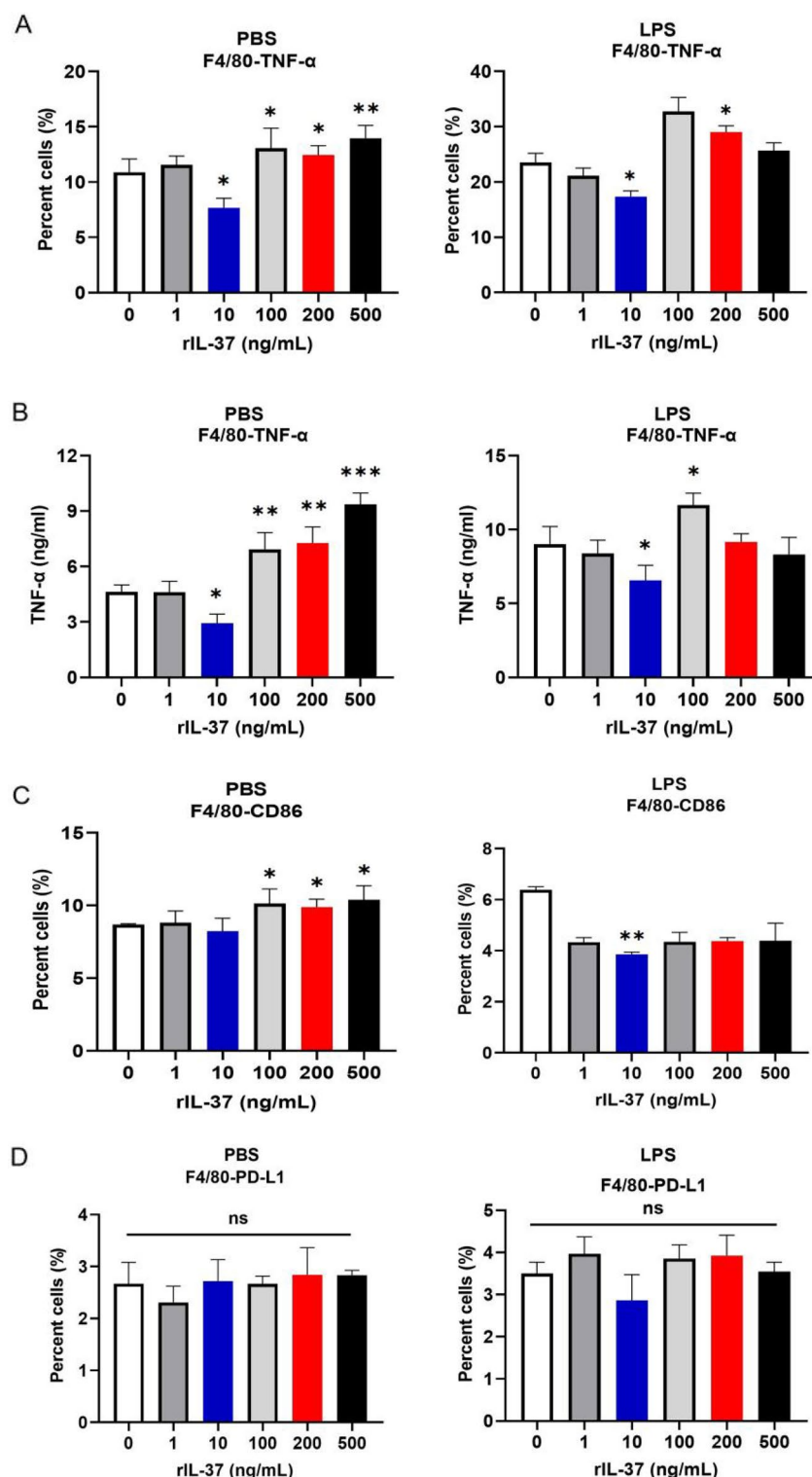


**Fig. 2.** High-dose rIL-37 stimulates macrophage activity. (A, B) Expression of F4/80-TNF- $\alpha$  increased in high-dose rIL-37 groups (100/200/500 ng/ml) and decreased in the low-dose rIL-37 group (10 ng/ml) before and after LPS stimulation by Flow cytometry and ELISA. (C) High doses (100, 200, and 500 ng/ml) of rIL-37 promoted the expression of F4/80-CD86 compared with low doses (1 and 10 ng/ml). (D) No significant change in F4/80-PD-L1 expression at different rIL-37 doses. vs. 0 ng/ml, \* $P < 0.05$ , \*\* $P < 0.01$ , ns: not significant.

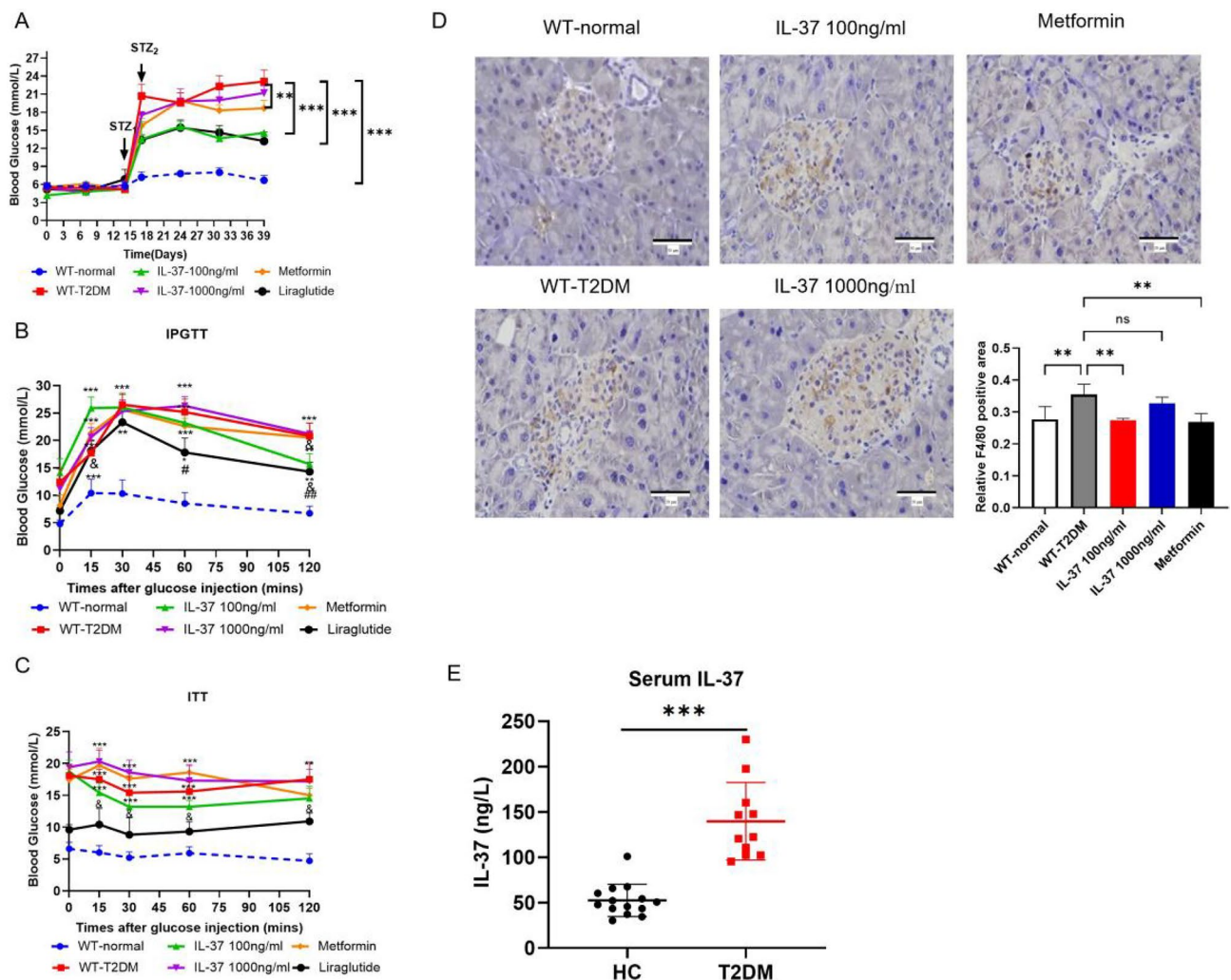


**Fig. 3.** High-dose rIL-37 could not reverse T2DM induced by HFD and STZ. (A) rIL-37 at 100 ng/ml concentration decreased the fasting blood glucose level of experimental T2D effectively, but 1000 ng/ml rIL-37 did not. (B, C) rIL-37 at 100 ng/ml concentration improved glucose tolerance (IPGTT) and insulin tolerance (ITT) effectively in experimental T2D, but 1000 ng/ml rIL-37 did not. (D) The 100 ng/ml rIL-37 effectively reduced immunohistochemical staining of F4/80-positive cells in islets of experimental T2DM but 1000 ng/ml rIL-37 can not. (Scale bar = 50  $\mu$ m). (E) Enhanced level of serum IL-37 in patients with T2DM compared with healthy controls. HC, healthy control; T2DM, type 2 diabetes mellitus. vs. WT-normal group, \* $P$ <0.05, \*\* $P$ <0.01, \*\*\* $P$ <0.001; vs. WT-T2DM, & $P$ <0.05; vs. IL-37 100 ng/ml, # $P$ <0.05, ## $P$ <0.01.

### Similar changes of signaling events in IL-37<sup>hi</sup>-TG macrophages

To further verify the mechanism of IL-37 acting on macrophages to regulate inflammation reaction in vivo, we isolated spleen macrophages from IL-37<sup>hi</sup>-TG and IL-37<sup>lo</sup>-TG mice and stimulated them with PBS and LPS, respectively. In IL-37<sup>lo</sup>-TG mice, p-STAT3 and p-AMPK $\alpha$  levels were significantly increased compared to WT mice at the condition of LPS, but decreased level of p-AMPK $\alpha$  and not changed level of p-STAT3 were observed in IL-37<sup>hi</sup>-TG mice (Fig. 5A and F), which confirmed almost similar signal events in vitro experiments. In addition, compared to WT mice, p-AKT, p-Erk, and p-NF- $\kappa$ B levels were significantly decreased in IL-37<sup>lo</sup>-TG mice at condition of LPS, but increased levels of p-AKT and p-Erk were observed in IL-37<sup>hi</sup>-TG mice (Fig. 5G and O). Moreover, the phosphatidylinositol-3 kinase-MAPK signaling pathway was also inhibited in IL-37<sup>lo</sup>-TG mice, but activation of this pathway was observed in IL-37<sup>hi</sup>-TG mice (Supplementary Fig.S10A).

### Discussion

The expression of IL-37 is closely related to T2DM. The level of IL-37 in the peripheral blood of elderly T2DM patients with insulin sensitivity is significantly higher than that of T2DM patients with insulin insensitivity and normal controls<sup>24</sup> which suggests that IL-37 may play a double-edged sword role in T2DM. This study prompted that high-dose IL-37 promotes inflammatory activity of macrophage via preferential ligation of the IL-18R $\alpha$ , and cannot reverse T2DM induced by HFD and STZ. At the same time, low-dose IL-37 has good therapeutic effect on T2DM. Overall, our current study revealed the double-edged sword effect of IL-37 treatment on the control



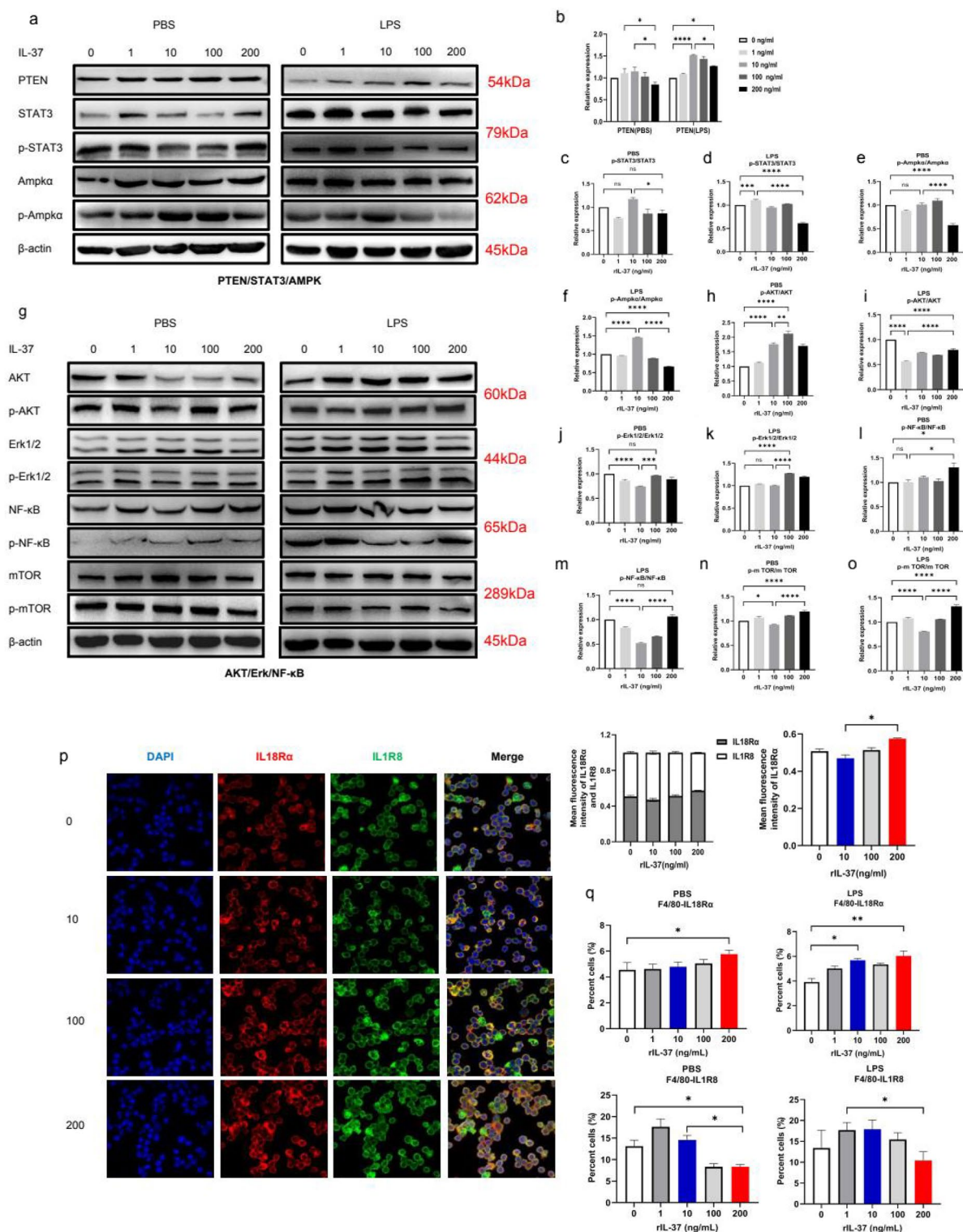


**Fig. 4.** High-dose rIL-37 inhibits STAT3 activation in macrophages. (A-F) High-dose rIL-37 (100 and 200 ng/ml) inhibited the activation of PTEN/STAT3/AMPK signaling pathway. (G-O) High-dose rIL-37 (100 and 200 ng/ml) activated the AKT/Erk/NF- $\kappa$ B/mTOR signaling pathway. (P) Results of Immunofluorescence showed that high-dose rIL-37 (200 ng/ml) preferentially ligate to IL-18Ra receptor instead of IL-1R8 receptor. (Q) Results of flow cytometry confirmed the immunofluorescence finding. \* $P < 0.05$ , \*\* $P < 0.01$ , \*\*\* $P < 0.001$ .



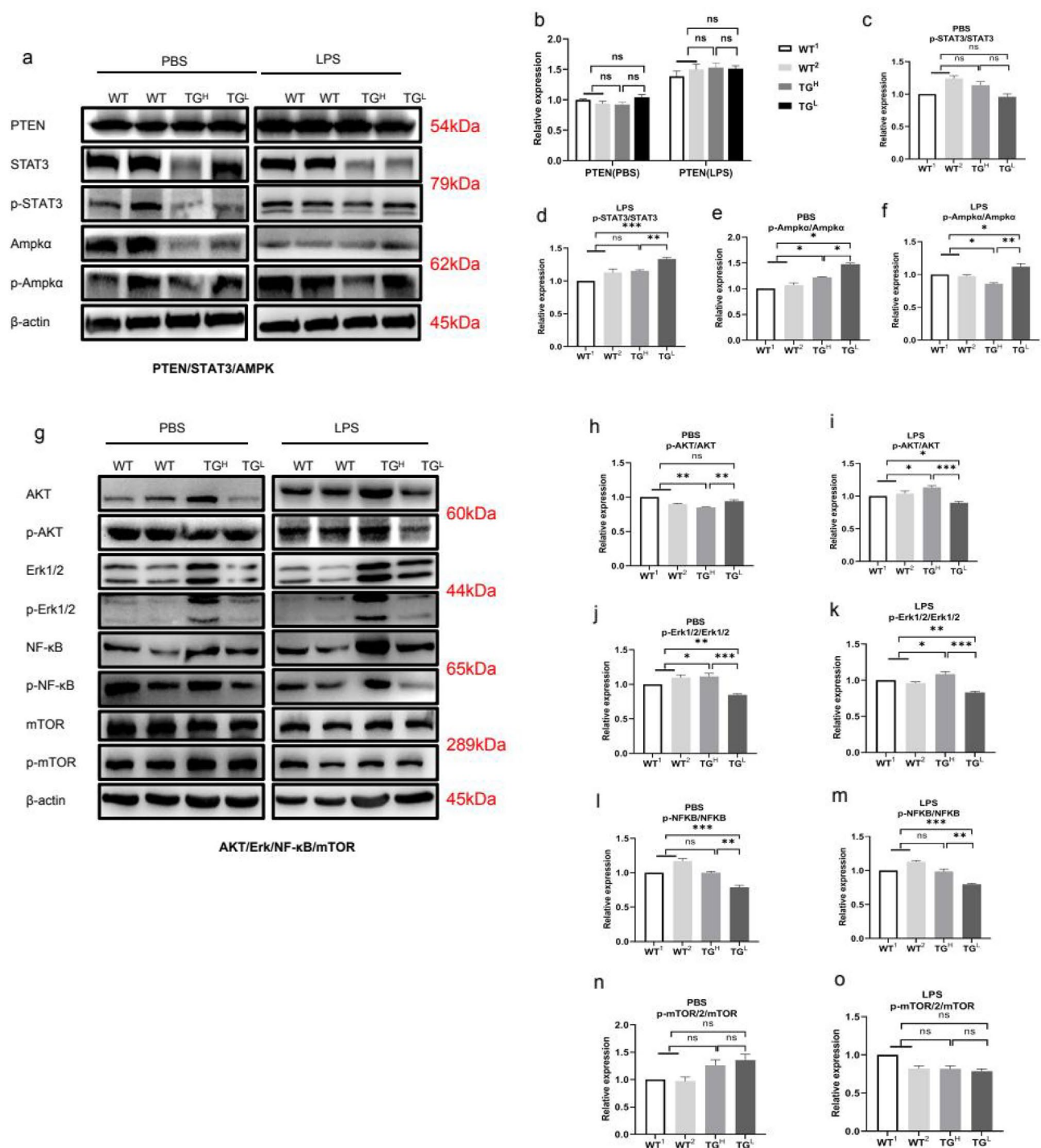


**Fig. 5.** Similar changes of signaling events in IL-37<sup>hi</sup>-TG macrophages. (A-F) Inhibited activation of AMPK was observed in IL-37<sup>hi</sup>-TG mice. (G-O) Activated AKT/Erk signaling pathway was confirmed in IL-37<sup>hi</sup>-TG mice. \**P* < 0.05, \*\**P* < 0.01, \*\*\**P* < 0.001.

of the inflammatory response of macrophages in T2DM via rIL-37 stimulation experiment in vitro and IL-37 TG mice experiment in vivo.

The expression of IL-37 in immune cells is mainly concentrated in DCs, circulating monocytes, plasma cells, tonsil B cells, and tissue macrophages<sup>33,34</sup>. Our study indicated that compared with IL-37<sup>lo</sup>-TG and WT mice, IL-37<sup>hi</sup>-TG mice showed increased frequency and activity of macrophages and CD8<sup>+</sup> T cells. At present, most studies have focused on the inhibitory changes in the immune cell activity of IL-37 TG mice, and a limited number have reported changes in the immune cells of IL-37 TG mice with different copy numbers. Suzhao Li et al. observed that compared with WT mice, the peritoneal macrophages of IL-37 TG mouse can reduce LPS-

induced proinflammatory cytokine expression effectively to 40–50%<sup>35</sup>. Compared with the WT mice, 60% fewer pro-inflammatory microglia-macrophages and fourfold higher expression of anti-inflammatory markers were detected in the ischemic hemisphere of IL-37 TG mice<sup>36</sup>. IL-37 dampened protective cytotoxic T cell-mediated immunity in colitis-associated colorectal cancer (CAC) and B16-OVA models. The number and activity of CD8 + T cells in IL-37 TG CAC model mouse decreased and failed to proliferate and produce cytotoxic cytokines; this condition enabled the tumor evasion of immune surveillance<sup>37</sup>. The difference between this study and previous studies is that differences in the number and activity of macrophages and CD8 + T cells were observed in IL-37 TG mice with high and low copy numbers, indicating that different doses of IL-37 have different effects on immune cells in the body.

In vitro, rIL-37 downregulates the expression of iNOS, CD11c, MCP-1, and IL-6 in M1 macrophages<sup>8,38</sup> and upregulates the expression of IL-10 and CD206 in M2 macrophages<sup>8</sup>. Thus, IL-37 can transform macrophage polarization from M1 phenotype (pro-inflammatory) to M2 phenotype (anti-inflammatory). Based on the above studies, this study further explored the effects of different doses of rIL-37 on macrophage activity in vitro. Our results showed that 10 ng/ml rIL-37 can inhibit the LPS-induced TNF- $\alpha$  and M1 macrophage marker CD86 effectively, whereas the inhibition of rIL-37 at the concentrations of 100, 200, and 500 ng/ml on LPS-induced proinflammatory cytokines disappeared or promoted the expressions of these cytokines. This result was partially similar to that of Li S et al.<sup>35</sup>, who observed that IL-37 precursors at picomolar concentrations optimally suppressed the production of TNF- $\alpha$ , IL-6, and IL-1 $\beta$  in human blood M1 macrophages; however, the study did not report the specific effect of high-dose IL-37. Our results further confirmed the double-edged sword effect of IL-37 on the anti-inflammatory process of macrophages in vitro.

IL-37 is associated closely with the occurrence and development of obesity and T2DM. Hailin Jia discovered that IL-37 expression in the subcutaneous adipose tissue of obese population was correlated negatively with body mass index, serum insulin, and homeostasis model assessment index<sup>39</sup>. After 16 weeks of high-fat diet feeding, compared with the WT mice, the IL-37 TG mice showed decreased weight gain, number of adipocytes, liver weight, and liver triglyceride content, and blood cholesterol level<sup>25</sup>. Dov B. Ballak et al. indicated that the anti-inflammatory effect of IL-37 can improve the established metabolic disturbances during obesity<sup>26</sup>. Tianyi Li et al. suggested that IL-37 suppressed the gut microbiota dysbiosis and was associated with highly insulin-sensitive elderly T2DM patients<sup>24</sup>. The above studies proved that IL-37 may have important therapeutic value in obesity-induced inflammation and insulin resistance through human specimens and mouse models. On the basis of constructing a T2DM mouse model with high-fat diet and streptozotocin (STZ), our team intervened by intraperitoneal injection of rIL-37 (100 and 1000 ng/mouse/week). The results showed that 100 ng/mouse/week intervention can reduce blood glucose and the number of islet macrophages and improve glucose and insulin tolerances effectively as well, whereas 1000 ng/mouse/week intervention did not improve the above indicators, which suggested that low-dose administration of IL-37 had a protective effect on T2DM, however, high dose IL-37 has no protective effect on diabetes.

The function of IL-37 is related to the formation of extracellular IL-37 dimers. rIL-37 at a very low concentration (1 mg/mouse in vivo or 0.1 ng/ml in vitro) is sufficient to exert its ideal and effective anti-inflammatory effect<sup>4,26</sup>. Nevertheless, a weak repression on the expression of inflammatory cytokines was observed when using high concentrations of IL-37 (100 ng/ml in vitro)<sup>29</sup>. This low-dose effect of IL-37 may have a bearing on the spontaneous born of IL-37 homodimers, which further restrict the bioactivity of IL-37 by blocking the IL-1R8 co-receptor recruitment or by lowering the steric affinity for IL-18R $\alpha$ <sup>40</sup>, which may be supposed to an self-regulation mechanism to limit over immunosuppression. In this experiment, the difference from the study of Ballak DB et al.<sup>26</sup> is that 100 ng/mouse/week IL-37 has a perfect protective effect on the T2DM model, while 1000 ng/mouse/week IL-37 has no effect on the T2DM model, suggesting that there may be differences in the dosage at which IL-37 plays a role in different disease models. Preliminary analysis of the mechanism suggests that high-dose IL-37 inhibits the recruitment of IL-1R8 and preferentially ligates to IL-18R $\alpha$  (but the steric affinity for IL-18R $\alpha$  may be lowered), which restricts the anti-inflammatory activity of IL-37 in macrophages, and is not conducive to the prognosis of diabetes.

Considering that mice lack an endogenous IL-37 homolog, we selected human IL-37 transgenic mice for the study. Through literature review, Nold-Petry et al.<sup>27</sup> confirmed through human IL-37 transgenic mice that IL-37 in human IL-37 transgenic mice could exert anti-inflammatory effects by binding to mouse IL-18R $\alpha$  and IL-1R8 (SIGIRR).

The role and mechanism of IL-37 in macrophage inflammatory response have been reported. IL-37 plays an inhibition role in macrophage polarization to M1 type by inhibiting the Notch1 and NF- $\kappa$ B pathways<sup>8</sup>. In macrophages, IL-37 regulates the activity of PTEN, NF- $\kappa$ B, and the expressions of cytokines, including IL-6, IL-1 $\beta$ , and IL-10<sup>12</sup>. In addition, IL-37 reduces pro-inflammatory cytokines in macrophages in a MAPK-dependent manner, thereby improving influenza pneumonia<sup>41</sup>. We confirmed in vivo and in vitro that low doses of IL-37 exerted a remarkable anti-inflammatory effect on macrophages and a protective effect on the T2DM model, while high doses of IL-37 have a certain degree of pro-inflammatory activity and have no protective effect on the T2DM model. Preliminary exploration of its mechanism suggests that low doses of IL-37 play an influential anti-inflammatory role in macrophages<sup>12</sup> via recruiting IL-1R8 more effectively and activating the PTEN/STAT3/AMPK signaling pathway, while inhibiting AKT/Erk/NF- $\kappa$ B/mTOR pathway, however, high doses of IL-37 plays a certain degree of proinflammatory role in macrophages by ligating to IL-18R $\alpha$  preferentially (may reduce the spatial affinity of IL-18R $\alpha$ ) and inhibiting PTEN/STAT3/AMPK pathway and activating AKT/Erk/NF- $\kappa$ B/mTOR pathway, which is not conducive to the outcome of diabetes. Conti P et al.<sup>42</sup> and Ballak DB<sup>43</sup> also confirmed the activation of AMPK and the repression of mTOR by IL-37<sup>44</sup>. Our research findings suggest that the double-edged sword role IL-37 in macrophage inflammatory response may be related to the opposite regulation of the above two signal pathways by different doses of IL-37. However, Moretti S et al. also used 100 and 1000 ng/mouse rIL-37 intraperitoneal injection to intervene with the acute pneumonia model and

observed reduced bronchoalveolar lavage fluid neutrophilia<sup>11</sup> alleviated neutrophil infection in the lung, and eased lung damage<sup>41</sup>. The different effects of various doses of IL-37 on various disease models may be related to the differences in disease models and their internal environment.

## Conclusion

In conclusion, these findings suggest that IL-37 has a double-edged sword effect on inflammatory responses in macrophages. Very low doses of IL-37 (10 ng/ml in vitro and 100 ng/mouse in vivo) are sufficient to induce excellent anti-inflammatory effects, whereas high-dose IL-37 inhibits the activation of PTEN, AMPK, and STAT3 via preferential connection to IL-18R and stimulates the pro-inflammatory activity of macrophages. These results highlight low-dose IL-37 as a potential therapeutic to ameliorate inflammation and metabolic disturbances during T2DM. However, high-dose IL-37 had no effect or had the opposite effect on T2DM. These results suggest that IL-37 sustained-release drugs can be developed for the treatment of T2DM in the future. The half-life of IL-37 in vivo and IL-18Ra knockout experiments need to be added in future research to further clarify the role and mechanism of different doses of IL-37 in the treatment of T2DM.

## Data availability

The data that support the findings of this study are available from the corresponding author Yu Zhang upon reasonable request.

Received: 11 March 2025; Accepted: 3 June 2025

Published online: 01 July 2025

## References

- Boraschi, D. et al. IL-37: a new anti-inflammatory cytokine of the IL-1 family. *Eur. Cytokine Netw.* **22**, 127–147 (2011).
- Bufler, P. et al. A complex of the IL-1 homologue IL-1F7b and IL-18-binding protein reduces IL-18 activity. *Proc. Natl. Acad. Sci. USA.* **99**, 13723–13728 (2002).
- Kumar, S. et al. Identification and initial characterization of four novel members of the interleukin-1 family. *J. Biol. Chem.* **275**, 10308–10314 (2000).
- Li, S. et al. Extracellular forms of IL-37 inhibit innate inflammation in vitro and in vivo but require the IL-1 family decoy receptor IL-18R. *Proc. Natl. Acad. Sci. USA.* **112**, 2497–2502 (2015).
- Dunn, E., Sims, J. E. & Nicklin, M. J. O'Neill, L. A. Annotating genes with potential roles in the immune system: six new members of the IL-1 family. *Trends Immunol.* **22**, 533–536 (2001).
- Busfield, S. J. et al. Identification and gene organization of three novel members of the IL-1 family on human chromosome 2. *Genomics* **66**, 213–216 (2000).
- Taylor, S. L., Renshaw, B. R., Garka, K. E., Smith, D. E. & Sims, J. E. Genomic organization of the interleukin-1 locus. *Genomics* **79**, 726–733 (2002).
- Zhou, P. et al. Interleukin 37 suppresses M1 macrophage polarization through Inhibition of the Notch1 and nuclear factor kappa B pathways. *Front. Cell. Dev. Biol.* **8**, 56 (2020).
- McCurdy, S., Baumer, Y., Toulmin, E., Lee, B. H. & Boisvert, W. A. Macrophage-Specific expression of IL-37 in hyperlipidemic mice attenuates atherosclerosis. *J. Immunol.* **199**, 3604–3613 (2017).
- McNamee, E. N. et al. Interleukin 37 expression protects mice from colitis. *Proc. Natl. Acad. Sci. USA.* **108**, 16711–16716 (2011).
- Moretti, S. et al. IL-37 inhibits inflammasome activation and disease severity in murine aspergillosis. *PLoS Pathog.* **10**, e1004462 (2014).
- Yang, Z. et al. Role of IL-37 in cardiovascular disease inflammation. *Can. J. Cardiol.* **35**, 923–930 (2019).
- Cavalli, G. et al. Treating experimental arthritis with the innate immune inhibitor interleukin-37 reduces joint and systemic inflammation. *Rheumatol. (Oxford)* **55**, 2220–2229 (2016).
- Ye, L. et al. IL-37 alleviates rheumatoid arthritis by suppressing IL-17 and IL-17-Triggering cytokine production and limiting Th17 cell proliferation. *J. Immunol.* **194**, 5110–5119 (2015).
- Bi, Y. et al. Contributing factors of fatigue in patients with type 2 diabetes: A systematic review. *Psychoneuroendocrinology* **130**, 105280 (2021).
- Pan, Y. et al. The role of IL-37 in skin and connective tissue diseases. *Biomed. Pharmacother.* **122**, 109705 (2020).
- Sun, H. et al. IDF diabetes atlas: global, regional and country-level diabetes prevalence estimates for 2021 and projections for 2045. *Diabetes Res. Clin. Pract.* **183**, 109119 (2022).
- Toejing, P., Khampithum, N., Sirilun, S., Chaayasut, C. & Lailerd, N. J. F. Influence of Lactobacillus paracasei HII01 Supplementation on Glycemia and Inflammatory Biomarkers in Type 2 Diabetes: A Randomized Clinical Trial. *Foods* **10**, 1455 (2021).
- Lan, Y. et al. Temporal relationship between atherogenic dyslipidemia and inflammation and their joint cumulative effect on type 2 diabetes onset: a longitudinal cohort study. *BMC Med.* **21**, 31 (2023).
- Mosterd, C. M. et al. Intestinal microbiota and diabetic kidney diseases: role of microbiota and derived metabolites in the modulation of renal inflammation and disease progression. *Best Pract. Res. Clin. Endocrinol. Metab.* **35**, 101484 (2021).
- Donath, M. Y. Targeting inflammation in the treatment of type 2 diabetes: time to start. *Nat. Rev. Drug Discov.* **13**, 465–476 (2014).
- Holt, A. et al. Heart failure following Anti-Inflammatory medications in patients with type 2 diabetes mellitus. *J. Am. Coll. Cardiol.* **81**, 1459–1470 (2023).
- Ye, L. et al. IL-37 inhibits the production of inflammatory cytokines in peripheral blood mononuclear cells of patients with systemic lupus erythematosus: its correlation with disease activity. *J. Transl. Med.* **12**, 69 (2014).
- Li, T. et al. Interleukin-37 sensitize the elderly type 2 diabetic patients to insulin therapy through suppressing the gut microbiota dysbiosis. *Mol. Immunol.* **112**, 322–329 (2019).
- Ballak, D. B. et al. IL-37 protects against obesity-induced inflammation and insulin resistance. *Nat. Commun.* **5**, 4711 (2014).
- Ballak, D. B. et al. Interleukin-37 treatment of mice with metabolic syndrome improves insulin sensitivity and reduces pro-inflammatory cytokine production in adipose tissue. *J. Biol. Chem.* **293**, 14224–14236 (2018).
- Nold-Petry, C. A. et al. IL-37 requires the receptors IL-18Ra and IL-18R (SIGIRR) to carry out its multifaceted anti-inflammatory program upon innate signal transduction. *Nat. Immunol.* **16**, 354–365 (2015).
- Li, C. et al. IL-37 isoform D acts as an inhibitor of soluble ST2 to boost type 2 immune homeostasis in white adipose tissue. *Cell. Death Discov.* **8**, 163 (2022).
- Eisenmesser, E. Z. et al. Interleukin-37 monomer is the active form for reducing innate immunity. *Proc. Natl. Acad. Sci. USA.* **116**, 5514–5522 (2019).
- Liu, Y., Deng, J. & Fan, D. Ginsenoside Rk3 ameliorates high-fat-diet/streptozocin induced type 2 diabetes mellitus in mice via the ampk/akt signaling pathway. *Food Funct.* **10**, 2538–2551 (2019).

31. Hongyu, Z., Lian, W., Xiaoyu, H. N., Hao, X. U. & Xiaotang, F. a. N. Metformin treatment during neonatal period rescues hippocampal neurogenesis in the BTBR T + Itpr3tf/J mouse model of autism. *Di-san Junyi Aaxue Xuebao*. **42**, 1–8 (2020).
32. Hansen, H. H. et al. The DPP-IV inhibitor linagliptin and GLP-1 induce synergistic effects on body weight loss and appetite suppression in the diet-induced obese rat. *Eur. J. Pharmacol.* **741**, 254–263 (2014).
33. Rudloff, I. et al. Monocytes and dendritic cells are the primary sources of Interleukin 37 in human immune cells. *J. Leukoc. Biol.* **101**, 901–911 (2017).
34. Cavalli, G. & Dinarello, C. A. Suppression of inflammation and acquired immunity by IL-37. *Immunol. Rev.* **281**, 179–190 (2018).
35. Li, S. et al. Role for nuclear interleukin-37 in the suppression of innate immunity. *Proc. Natl. Acad. Sci. USA*. **116**, 4456–4461 (2019).
36. Zhang, S. R. et al. IL-37 increases in patients after ischemic stroke and protects from inflammatory brain injury, motor impairment and lung infection in mice. *Sci. Rep.* **9**, 6922 (2019).
37. Wang, Z. et al. Interleukin-37 promotes colitis-associated carcinogenesis via SIGIRR-mediated cytotoxic T cells dysfunction. *Signal. Transduct. Target. Ther.* **7**, 19 (2022).
38. Luo, P., Peng, S., Yan, Y., Ji, P. & Xu, J. IL-37 inhibits M1-like macrophage activation to ameliorate temporomandibular joint inflammation through the NLRP3 pathway. *Rheumatol. (Oxford)*. **59**, 3070–3080 (2020).
39. Moschen, A. R. et al. Adipose and liver expression of Interleukin (IL)-1 family members in morbid obesity and effects of weight loss. *Mol. Med.* **17**, 840–845 (2011).
40. Ellisdon, A. M. et al. Homodimerization attenuates the anti-inflammatory activity of interleukin-37. *Sci. Immunol.* **2**, eaaj1548 (2017).
41. Qi, F. et al. Interleukin-37 ameliorates influenza pneumonia by attenuating macrophage cytokine production in a MAPK-Dependent manner. *Front. Microbiol.* **10**, 2482 (2019).
42. Conti, P. et al. Induction of pro-inflammatory cytokines (IL-1 and IL-6) and lung inflammation by Coronavirus-19 (COVI-19 or SARS-CoV-2): anti-inflammatory strategies. *J. Biol. Regul. Homeost. Agents*. **34**, 327–331 (2020).
43. Ballak, D. B. et al. Short-term interleukin-37 treatment improves vascular endothelial function, endurance exercise capacity, and whole-body glucose metabolism in old mice. *Aging Cell*. **19**, e13074 (2020).
44. Nold, M. F. et al. IL-37 is a fundamental inhibitor of innate immunity. *Nat. Immunol.* **11**, 1014–1022 (2010).

## Author contributions

Gong. Lu. and Zhang.: the conception and design of the study. Shi. Bi. Li. Wu. Wu. and Qiu.: acquisition of data, analysis and interpretation of data. Zhang. and Shi.: wrote the main manuscript text, prepared figures, statistical analysis. Zhang. and Lin.: methodology; Gong. and Lu.: Supervision. All authors contributed to the article and approved the submitted version.

## Funding

This work was supported by the National Natural Science Foundation of China (82100870).

## Declarations

## Competing interests

The authors declare no competing interests.

## Disclosure

Yu Zhang and Beixi Shi should be considered joint first authors.

## Conflict of interest

The author has no potential conflicts of interest.

## Additional information

**Supplementary Information** The online version contains supplementary material available at <https://doi.org/10.1038/s41598-025-05623-8>.

**Correspondence** and requests for materials should be addressed to Y.Z. or W.G.

**Reprints and permissions information** is available at [www.nature.com/reprints](http://www.nature.com/reprints).

**Publisher's note** Springer Nature remains neutral with regard to jurisdictional claims in published maps and institutional affiliations.

**Open Access** This article is licensed under a Creative Commons Attribution-NonCommercial-NoDerivatives 4.0 International License, which permits any non-commercial use, sharing, distribution and reproduction in any medium or format, as long as you give appropriate credit to the original author(s) and the source, provide a link to the Creative Commons licence, and indicate if you modified the licensed material. You do not have permission under this licence to share adapted material derived from this article or parts of it. The images or other third party material in this article are included in the article's Creative Commons licence, unless indicated otherwise in a credit line to the material. If material is not included in the article's Creative Commons licence and your intended use is not permitted by statutory regulation or exceeds the permitted use, you will need to obtain permission directly from the copyright holder. To view a copy of this licence, visit <http://creativecommons.org/licenses/by-nc-nd/4.0/>.

© The Author(s) 2025